Optimal control of Tollmien–Schlichting waves in a developing boundary layer

Steeve Walther, Christophe Airiau, and Alessandro Bottaro
Institut de Mécanique des Fluides de Toulouse, Allée du Professeur Camille Soula, 31400 Toulouse, France

(Received 28 June 2000; accepted 19 March 2001)

Optimal control theory is used to determine the wall transpiration (unsteady blowing/suction) with zero net mass flux capable of attenuating Tollmien–Schlichting waves in a spatially developing boundary layer. The flow state is determined from the parabolized stability equations, in a linear setting. An appropriate cost functional is introduced and minimized iteratively by the numerical solution of the equations for the state and the dual state, coupled via transfer and optimality conditions. Central to the control is the determination of the wall Green's function expressing the receptivity of the flow to wall inhomogeneities. The optimal wall velocity is obtained in few iterations and a reduction of several orders of magnitude in output disturbance energy is demonstrated, as compared to the uncontrolled case, for control laws operating both over the whole wall length and over a finite strip. Finally, white noise disturbances are applied to the optimal wall velocities already determined, to assess the influence of an imperfectly operating controller on the final result, and to decide on the practical feasibility of the approach. © *2001 American Institute of Physics.* [DOI: 10.1063/1.1378035]

I. INTRODUCTION

The capacity of influencing a given flow to make it behave according to a predetermined goal is clearly an endeavor of fundamental as well as technological significance. In aeronautics much research effort is being spent on finding feasible ways to manipulate the boundary layers over wings, fins, and nacelles, to delay transition to turbulence and, consequently, reduce the skin friction, as compared to the uncontrolled situation. Skin friction drag accounts for some 50% of the total drag in large civil transport aircraft, and the ability to reduce it presents clear economic and environmental advantages. The active technology by which the boundary layer is manipulated to pursue a desired objective is called laminar flow control (LFC).

Industrial and academic efforts in LFC so far have mainly concentrated on the determination of a steady wall suction distribution capable of delaying the onset of transition. A large amount of literature exists, comprehensively reviewed by Joslin.[1,2] Flow manipulation is one of the areas in which optimal control theory finds its application: an objective functional is specified and manners of extremizing it are proposed, possibly relying on the determination of sensitivities or on the solution of an adjoint problem.[3] (A sensitivity function is defined as the gradient of the flow state with respect to a control variable.) In LFC the objective is to provoke an order one change in the base flow in such a way that the new base flow produced is less prone to destabilization. The classical argument is that suction through a porous surface or a slot produces a thinner boundary layer characterized by a smaller shape factor, in which the growth of Tollmien–Schlichting (TS) waves is postponed. On the negative side, a thinner boundary layer has larger skin friction, which contradicts the desired goal of drag reduction. Furthermore, if the flow is swept (as often occurs in aeronautical applications), the effect of suction on the cross-flow instability is less understood. These (sometime) opposing requirements in the search for the optimal suction distribution are to be expressed mathematically as an appropriate cost functional; then, the optimization problem yields the optimal solution for any desired flow configuration and parameter setting.

A somewhat different perspective to control is adopted here: rather than focusing on modifications to the mean flow, the control efforts are aimed at the unstable mode itself. This technique, which goes by the name of wave cancellation or wave superposition, has advantages and disadvantages. The main drawback is that the instability wave must be determined, possibly by micro-sensors positioned in the flow. The output from the sensors must then be fed onto a state evaluator that produces an estimate of the wave (shape, amplitude and phase), at which point the (boundary) control might operate. One of the advantages is that effective control laws might be predefined for a variety of instability modes, possibly creating a database that could be rapidly accessed by a controller. Another advantage is that by acting on a small (order ϵ) perturbation, only a very small amount of control energy (order ϵ^2) must be provided to efficiently damp the wave.

Experimental work on the wave superposition concept in boundary layers was initiated at Lockheed by Milling;[4] he performed experiments in water and used an oscillating wire both to induce the wave and to suppress it. Subsequent studies employed heating elements,[5–8] vibrating ribbons,[9–11] sound from a loudspeaker,[7,12] surface deflection,[13] and periodic blowing/suction through slots or rows of holes.[13] All investigations achieved some degree of success in reducing the wave amplitude, but none was able to achieve complete

antiphase control; the primary wave amplitude was reduced at the most by one order of magnitude and, eventually, the residual disturbance left in the flow brought about transition via three-dimensional interaction mechanisms. Hence, the realization came about that efforts at damping the primary disturbance alone might not suffice for significant transition delay, unless the control was applied right at the beginning of the primary disturbance's amplification phase. This was an early recognition of the importance of the receptivity process.

In theory, a complete elimination of the primary instability wave—to significantly postpone transition avoiding the emergence of three-dimensional interactions—is possible. Recent theoretical work was conducted by Joslin and collaborators,[14–16] Bewley and Liu,[17] Cathalifaud and Luchini,[18] and Corbett.[19] Joslin *et al.*[16] determined the optimal boundary control for nonlinear TS waves in wall-bounded shear flows by an adjoint method arising from a Lagrangian optimization procedure applied to the Navier–Stokes system of equations. Bewley and Liu[17] used an optimal and a robust control approach for the damping of modes and pseudo-modes in a channel. Cathalifaud and Luchini[18] focused on the optimal control of streaks in a boundary layer, and of vortices developing along a concave wall because of the Görtler instability mechanism. They adopted a Lagrangian approach based on the three-dimensional boundary layer equations, an appropriate model when dealing with asymptotically elongated (along the streamwise direction) flow structures. An analogous procedure was followed by Corbett,[19] who studied the optimal control of modes and pseudo-modes in two- and three-dimensional boundary layers, using the temporal, parallel framework for the stability analysis.

In the present work, the search for optimal boundary control strategies is performed for a spatially developing two-dimensional boundary layer susceptible to destabilization by small amplitude TS waves. The approach is based on the parabolized stability equations (PSE);[20–24] this system permits a very rapid iterative search of the flow state and it can be easily extended to deal with nonlinear effects. To our knowledge this is the first article dealing with optimal control based on the, by now popular and well-established, PSE method. It provides an assessment on the possibilities of the PSE of being used in an iterative optimization procedure for instability control purposes.

One important aspect of the optimal control approach adopted here is that the initial, forcing condition may be arbitrary. The optimal, distributed control determined will be the appropriate one for the initial condition provided, which must hence be accurately known. An investigation on the receptivity properties of boundary layers constitutes the prerequisite step for the search of efficient flow management strategies. The adjoint method of receptivity analysis provides the Green's functions which directly quantify the efficiency of given forcing terms (at the wall or throughout the flow) in exciting instability waves.[21,25–29] For example, the forced receptivity to unsteady wall roughness can be properly defined via one adjoint calculation; the result of the calculation provides the wall Green's function which must be scalarly multiplied by any (arbitrary) wall inhomogeneity to yield the final amplitude of the instability wave. It is not a coincidence that these very Green's functions are central to the optimal control of the instability, as will be elucidated below.

II. DETERMINATION OF THE FLOW DISTURBANCE STATE

For the determination of the disturbance state the PSE approximation is employed; this technique's potential for nonlocal transition prediction studies in simple as well as more complex configurations has been demonstrated in a number of works.[21,30] The present application is limited to the case of two-dimensional TS waves in a Blasius boundary layer; its purpose is to show the feasibility of the control approach and to pave the way to further studies in more realistic configurations of aeronautical interest, for both LFC and wave cancellation approaches.

The flow is defined in a semi-infinite domain along the direction y normal to the wall, and between x_0 and x_f along the streamwise direction; lengths are scaled by $\delta_0 = (\nu x_0 / U_\infty)^{1/2}$ and velocities by U_∞, the free-stream velocity, with ν the kinematic viscosity. These scales define a Reynolds number R. The disturbance vector $\tilde{\mathbf{q}}$, comprising the velocity vector $\tilde{\mathbf{u}} = (\tilde{u}, \tilde{v})$ and the pressure $\tilde{p}$, is decomposed into an amplitude part and a time-dependent wave-like part as

$$\tilde{\mathbf{q}}(x,y,t) = \mathbf{q}(x,y)\chi(x)\exp[-i\omega t],$$

$$\chi(x) = \exp\left[i\left(\int_{x_0}^{x} \alpha(x')\,dx' \right) \right], \tag{1}$$

with α the complex wave number and ω the (real) wave frequency. In the following we note with $\hat{\mathbf{q}} = \chi\mathbf{q}$ the spatial part of the disturbance. The idea behind this decomposition stems from Wentzel–Kramers–Brillouin (WKB) analysis: one part of the disturbance ($\mathbf{q}$) is slowly varying in x, while the other (χ) varies rapidly, the two streamwise length scales being related by a small parameter which can be shown to scale with the inverse of R. As opposed to the WKB analysis, different orders in powers of the small parameter are not separated, but the first two orders are merged, thus yielding a partial differential system which contains the local and the nonlocal (to first order) approximations.[22,31] The advantage of the approach is that the resulting system (often appropriately *fixed*[31,32]) is parabolic and can be solved very efficiently.

In symbolic form the system reads

$$\chi\mathcal{L}_{\mathrm{PSE}}\mathbf{q} = 0$$

with

$$\mathcal{L}_{\mathrm{PSE}} = \left\{ \mathcal{A}\frac{\partial}{\partial y} + \mathcal{B}\frac{\partial}{\partial x} + \mathcal{C} + \mathcal{D}\frac{\partial^2}{\partial y^2} \right\}, \tag{2}$$

$$\int_0^\infty \overline{u}\frac{\partial u}{\partial x}\,dy = 0. \tag{3}$$

The latter equation, the so-called ''normalization'' condition, ensures that the growth of the wave is accounted for in the function χ; this condition provides the means of determining the unknown α. Different choices can be made with little (order R^{-1}) effect on the growth rate of the instability.[31] Overbar denotes complex conjugation, and the full form of the matrices is given in the Appendix.

Initial conditions can be specified from the local stability eigenproblem,

$$\alpha(x_0)=\alpha_0 \quad \text{and} \quad \mathbf{q}(x_0,y)=\mathbf{q}_0(y),$$

although this is not a necessary requirement and Herbert[33] has shown examples on the use of the PSE for algebraically (and transiently) growing disturbances.

Boundary conditions, including the control at the wall accomplished via a nonzero, time-harmonic vertical velocity [cf. Eq. (1)], read

$$u(x,0)=0; \quad \hat{v}_w(x)=v(x,0)\chi(x)=v_w\chi; \quad \lim_{y\to\infty}\mathbf{u}(x,y)=0.$$

Our problem is the determination of the optimal $\hat{v}_w$ which extremizes a given objective functional, subject to the constraints provided by the state equations with their initial and boundary conditions. From the physical point of view, the simplest thing one might wish to minimize is the disturbance energy, while providing a bound on the energy required to control the system. A convenient measure of the disturbance energy is

$$E(x)=\int_0^\infty \overline{\hat{u}}\hat{u}\,dy. \tag{4}$$

The control energy E_w can be simply related to the wall blowing/suction via

$$E_w=\int_{x_0}^{x_f}\overline{\hat{v}_w}\hat{v}_w\,dx. \tag{5}$$

An objective functional acting on the real range, and based on the final value of the perturbation energy, can then be defined

$$\mathcal{J}_0(\hat{u},\hat{v}_w,\alpha)=E(x_f)+\beta_w E_w. \tag{6}$$

Clearly other (more complex) choices can be made, although the functional proposed will suffice for the present purposes. The real coefficient β_w permits us to scale the relative influence of the two components of the cost. For example, choosing $\beta_w=0$ implies that the cost of the controller is not an issue, and the goal is just the minimization of the final disturbance energy. This is possibly a sensible choice, given that the control energy is minute anyway and scales with the square of the disturbance amplitude factor.

III. OPTIMAL CONTROL THEORY: THE DUAL STATE

The technique adopted here to solve the minimization problem is based on the Lagrange multipliers method, as discussed, for example, in the recent review article by Gunzburger[3] (see also references therein). The constrained optimization problem is transformed into an unconstrained optimization problem for an augmented, Lagrangian functional $\mathcal{L}$. This new functional, which also operates on the real range, takes directly into account the state equations and the inhomogeneous (unknown) wall boundary condition. There is no need to include the wall boundary condition on u, nor the free-stream condition on $\mathbf{u}$, since these quantities are, by construction, not subject to variations. All arguments in this new functional are assumed independent of one another. We have

$$\mathcal{L}(\mathbf{q},\hat{v}_w,\alpha,\hat{\mathbf{p}},\hat{\lambda},\gamma)=\mathcal{J}_0-\mathcal{J}_1,$$

with

$$\begin{aligned}\mathcal{J}_1=&\int_{x_0}^{x_f}\int_0^\infty \overline{\hat{\mathbf{p}}\chi}\mathcal{L}_{\mathrm{PSE}}\mathbf{q}\,dy\,dx\\&+\int_{x_0}^{x_f}\overline{\hat{\lambda}(x)}(\chi v(x,0)-\hat{v}_w)\,dx\\&+\int_{x_0}^{x_f}\overline{\gamma}(x)\int_0^\infty \overline{u}\frac{\partial u}{\partial x}\,dy\,dx+\text{c.c.},\end{aligned} \tag{7}$$

c.c. denoting complex conjugates.

The complex vector $\hat{\mathbf{p}}(x,y)$ and the complex functions $\hat{\lambda}(x)$ and $\gamma(x)$ are the Lagrange multipliers for the problem; they play the role of adjoint (or dual) variables for, respectively $\hat{\mathbf{q}}$, $\hat{v}_w$, and α. A recent study[34] has shown that $\hat{\mathbf{p}}$ and $\hat{\lambda}$ are more conveniently written in a manner similar to the direct variables, i.e., by the introduction of a wave-like part:

$$\hat{\mathbf{p}}(x,y)=\mathbf{p}(x,y)\chi^*(x), \quad \hat{\lambda}(x)=\lambda(x)\chi^*(x),$$

$$\chi^*(x)=\exp\left[i\left(\int_{x_f}^{x}\overline{\alpha}(x')dx'\right)\right].$$

A necessary condition for a minimum of the Lagrangian is that its variations with respect to each independent argument vanish; this requirement is expressed by employing Fréchet differentiation in the (generic) direction δa, e.g.,

$$\frac{\partial\mathcal{L}}{\partial a}\delta a=\lim_{\epsilon\to0}\frac{\mathcal{L}(a+\epsilon\delta a)-\mathcal{L}(a)}{\epsilon}.$$

Hence, the variation of the functional reads

$$\begin{aligned}\delta\mathcal{L}=&\frac{\partial\mathcal{L}}{\partial\mathbf{q}}\delta\mathbf{q}+\frac{\partial\mathcal{L}}{\partial\hat{v}_w}\delta\hat{v}_w+\frac{\partial\mathcal{L}}{\partial\alpha}\delta\alpha+\frac{\partial\mathcal{L}}{\partial\mathbf{p}}\delta\mathbf{p}+\frac{\partial\mathcal{L}}{\partial\lambda}\delta\lambda\\&+\frac{\partial\mathcal{L}}{\partial\gamma}\delta\gamma=0.\end{aligned}$$

All the different directional derivatives (the Lagrangian gradient) given below must vanish; their derivation, which requires a series of integration by parts to try and factorize the variations $\delta\mathbf{q}$, $\delta\hat{v}_w$, $\delta\alpha$, $\delta\mathbf{p}$, $\delta\lambda$, and $\delta\gamma$ within the integrals, is tedious but straightforward:

$$\frac{\partial \mathcal{L}}{\partial \mathbf{q}}\delta\mathbf{q}=\int_{x_0}^{x_f}\int_0^{\infty}\left(\chi_f\left\{\frac{\partial\overline{\mathbf{p}}\mathcal{A}}{\partial y}+\frac{\partial\overline{\mathbf{p}}\mathcal{B}}{\partial x}-\overline{\mathbf{p}}\mathcal{C}-\frac{\partial^2\overline{\mathbf{p}}\mathcal{D}}{\partial y^2}\right\}\delta\mathbf{q}\right.$$
$$\left.+\left[-\overline{\chi}_f\gamma\frac{\partial\overline{u}}{\partial x}+\chi_f\frac{\partial\overline{\gamma u}}{\partial x}\right]\delta u\right)dydx$$
$$-\int_{x_0}^{x_f}\left\{\chi_f\left[\overline{\mathbf{p}}\mathcal{A}\delta\mathbf{q}+\overline{\mathbf{p}}\mathcal{D}\frac{\partial\delta\mathbf{q}}{\partial y}-\frac{\partial\overline{\mathbf{p}}\mathcal{D}}{\partial y}\delta\mathbf{q}\right]_{y=0}^{\infty}\right.$$
$$\left.+\overline{\lambda}\chi\delta v\right\}dx+\chi_f\int_0^{\infty}\{\overline{\chi u}\delta u-\overline{\gamma u}\delta u-\overline{\mathbf{p}}\mathcal{B}\delta\mathbf{q}\}_{x=x_f}$$
$$\times dy+\text{c.c.},$$

$$\frac{\partial \mathcal{L}}{\partial \hat{v}_w}\delta\hat{v}_w=\int_{x_0}^{x_f}(\beta_w\overline{\hat{v}}_w+\overline{\lambda})\,\delta\hat{v}_w dx+\text{c.c.},$$

$$\frac{\partial \mathcal{L}}{\partial \alpha}\delta\alpha=iE_f\int_{x_0}^{x_f}\delta\alpha\,dx'$$
$$-\chi_f\int_0^{\infty}\int_{x_0}^{x_f}\overline{\mathbf{p}}\left(\frac{\partial\mathcal{L}_{\text{PSE}}}{\partial\alpha}\mathbf{q}\delta\alpha+\frac{\partial\mathcal{L}_{\text{PSE}}}{\partial\alpha'}\mathbf{q}\delta\alpha'\right)$$
$$\times dxdy-\int_{x_0}^{x_f}\overline{\lambda i\chi v}(x,0)\left(\int_{x_0}^{x}\delta\alpha\,dx'\right)dx+\text{c.c.},$$

$$\frac{\partial \mathcal{L}}{\partial \mathbf{p}}\delta\mathbf{p}=\chi_f\int_{x_0}^{x_f}\int_0^{\infty}\delta\overline{\mathbf{p}}\mathcal{L}_{\text{PSE}}\mathbf{q}\,dydx+\text{c.c.},$$

$$\frac{\partial \mathcal{L}}{\partial \lambda}\delta\lambda=\chi_f\int_{x_0}^{x_f}\delta\overline{\lambda}(v(x,0)-v_w)\,dx+\text{c.c.},$$

$$\frac{\partial \mathcal{L}}{\partial \gamma}\delta\gamma=\int_{x_0}^{x_f}\delta\overline{\gamma}\int_0^{\infty}\overline{u}\frac{\partial u}{\partial x}dydx+\text{c.c.},$$

with $\chi_f=\chi(x_f)=\overline{\chi}^*(x)\chi(x)$; $E_f=E(x_f)$; and $\alpha'=d\alpha/dx$.

Since all variations are arbitrary, except at boundaries where the conditions are fixed (such as, for example, at $x=x_0$), the different integrals vanish if the following Euler–Lagrange equations are satisfied:

$$\frac{\partial\mathcal{A}^*\mathbf{p}}{\partial y}+\frac{\partial\mathcal{B}^*\mathbf{p}}{\partial x}-\mathcal{C}^*\mathbf{p}-\frac{\partial^2\mathcal{D}^*\mathbf{p}}{\partial y^2}=\left\{\frac{\chi_f}{\overline{\chi}_f}\overline{\gamma}\frac{\partial u}{\partial x}-\frac{\partial\gamma u}{\partial x}\right\}(1,0,0)^T,\tag{8}$$

$$\lim_{y\to\infty}\mathbf{u}^*(x,y)=0,\tag{9}$$

$$\mathbf{u}^*(x,0)=0,\tag{10}$$

$$\lambda=\chi^*(x)p^*(x,0)=\hat{p}_w^*(x),\tag{11}$$

$$\mathcal{B}_f^*\mathbf{p}_f=(\chi_f-\gamma_f)u(x_f,y)(1,0,0)^T,\tag{12}$$

$$\lambda=-\beta_w\hat{v}_w,\tag{13}$$

$$\frac{\partial}{\partial x}\tilde{J}(\hat{\mathbf{p}},\hat{\mathbf{q}};x)=\hat{v}_w\overline{\hat{p}_w^*}=\chi_f v_w\overline{p_w^*},\tag{14}$$

$$E_f=\tilde{J}(\hat{\mathbf{p}}_f,\hat{\mathbf{q}}_f;x_f),\tag{15}$$

with

$$\tilde{J}(\hat{\mathbf{p}},\hat{\mathbf{q}};x)=\int_0^{\infty}\left[\overline{\hat{\mathbf{p}}\mathcal{D}}\frac{\partial\hat{\mathbf{q}}}{\partial x}-\frac{\partial\overline{\hat{\mathbf{p}}}}{\partial x}\mathcal{D}\hat{\mathbf{q}}+\overline{\hat{\mathbf{p}}\mathcal{B}}\hat{\mathbf{q}}\right]dy.\tag{16}$$

The matrices $\mathcal{A}^*$, $\mathcal{B}^*$, $\mathcal{C}^*$, and $\mathcal{D}^*$ in the adjoint PSE are given in the Appendix, and the subscript f beside a variable indicates its value at x_f.

The set of direct equations on $(\mathbf{q},\alpha)=(u,v,p,\alpha)$ and dual equations on $(\mathbf{p},\gamma)=(u^*,v^*,p^*,\gamma)$ need to be solved together with the normalization conditions (3) and (14) which allow for the determination of α and γ. The equations are coupled via the transfer conditions

$$\begin{aligned}&u^*(x_f,y)=0,\quad v^*(x_f,y)=0,\\&p^*(x_f,y)=(\chi_f-\gamma_f)u(x_f,y),\end{aligned}\tag{17}$$

$$\gamma_f\int_0^{\infty}u(x_f,y)\overline{u}(x_f,y)\,dy=\frac{1}{\mathrm{R}}\int_0^{\infty}\left\{\frac{\partial v^*}{\partial x}\overline{v}\right\}_{x=x_f}dy,\tag{18}$$

which apply at x_f. Equation (18) arises from the integration of Eq. (12) weighted by $\overline{\chi}_f\overline{\mathbf{q}}$ and from Eqs. (15) and (16). A simple order of magnitude analysis shows that $\gamma_f\approx\mathcal{O}(1/\mathrm{R}^2)$; γ_f is chosen equal to zero in the first loop, and then updated during the iterative process. Equations (17) and (18) represent the terminal conditions for the dual system, which is backward parabolic and for which the only direction of stable evolution is that of decreasing values of x. The determination of the control is made by the use of the optimality condition [cf. Eqs. (11) and (13)]:

$$\hat{v}_w=-\frac{1}{\beta_w}\hat{p}_w^*(x),\tag{19}$$

which relates the optimal boundary control to the adjoint variable $\hat{p}_w^*(x)$. The latter is precisely the Green's function defining the receptivity of the boundary layer to vertical velocity disturbances at $y=0$.[27–29,34] A beginning source on adjoint PSE for receptivity and control purposes is Hill.[35,36]

IV. THE OPTIMALITY SYSTEM AND ITS ITERATIVE RESOLUTION

A. The algorithm

The co-state (u^*,v^*,p^*,γ) is defined by Eq. (8) in the domain $[x_0,x_f]\times[0,\infty]$, by the closure relation on $\gamma(x)$ [Eq. (14)], by the terminal conditions at x_f [Eqs. (17) and (18)], plus homogeneous boundary conditions for $\mathbf{u}^*$ at the wall and for $y\to\infty$.

The optimality system linking direct and adjoint equations can be solved iteratively via a simple gradient method. The algorithm chosen follows the steps outlined below:

(i) Step 1: Solution of the local stability problem to initialize the PSE.
(ii) Step 2: Iteration $k=1$, $\hat{v}_w^{(1)}=0$.
(iii) Step 3: Solution of the direct state [Eqs. (2) and (3)] with inhomogeneous (except for $k=1$) wall condition on $\hat{v}$.

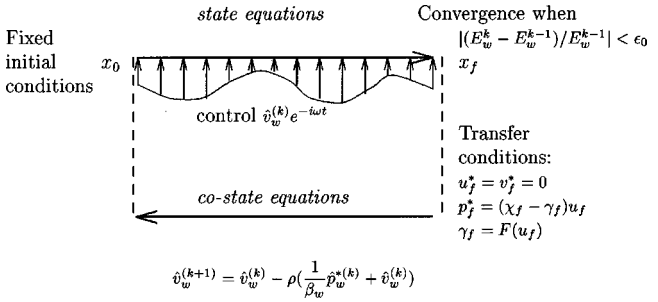

FIG. 1. Schematic of the optimal control algorithm.

(iv) Step 4: Evaluation of the terminal conditions $(\hat{\mathbf{p}}, \gamma)$ of the dual state via Eqs. (17) and (18). In (18), the value of $\mathbf{u}^*$ is that at the iteration $k-1$. For $k=1$, γ_f is set equal to zero.

(v) Step 5: Solution of the dual state [Eqs. (8–10) and (14)] by backward marching.

(vi) Step 6: Update of the blowing/suction distribution by the use of the relation

$$\hat{v}_w^{(k+1)} = \hat{v}_w^{(k)} - \rho\left(\frac{1}{\beta_w}\hat{p}_w^{*(k)} + \hat{v}_w^{(k)}\right),$$

where ρ is a relaxation factor; the expression in parenthesis represents (up to the multiplicative factor β_w) the gradient of the cost $\mathcal{J}_0$ with respect to the control $\hat{v}_w$.

(vii) Step 7: Convergence test on the control energy, i.e., if $|(E_w^k - E_w^{k-1})/E_w^{k-1}| < \epsilon_0$, then stop, else $k = k+1$, go to step 3. The convergence factor ϵ_0 is chosen equal to 10^{-4}.

A schematic of the algorithm is provided in Fig. 1. Although no efforts are made to optimize the relaxation factor ρ, convergence is very rapid and takes in general few iterations. The parameter β_w is chosen in such a way that the two terms in the cost function do not differ too much.

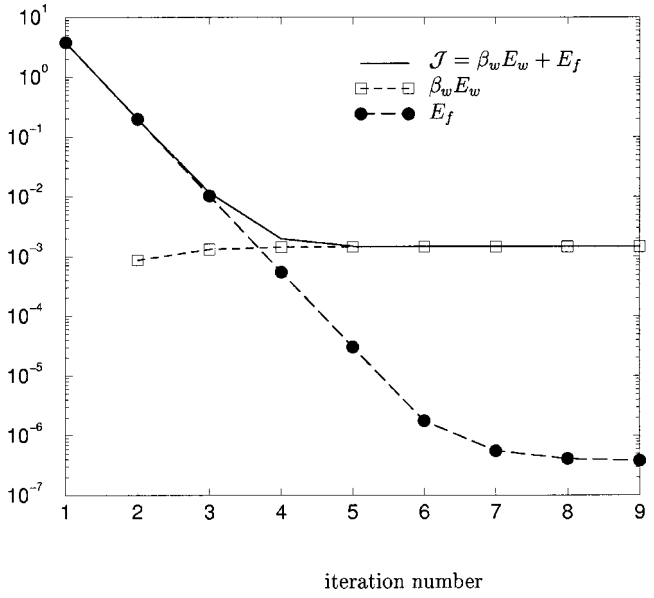

FIG. 2. Behavior of the cost functional and its components during the iterative process; $F=30$, $\beta_w = \beta_w^0$, $\rho = 3\times10^{-4}$.

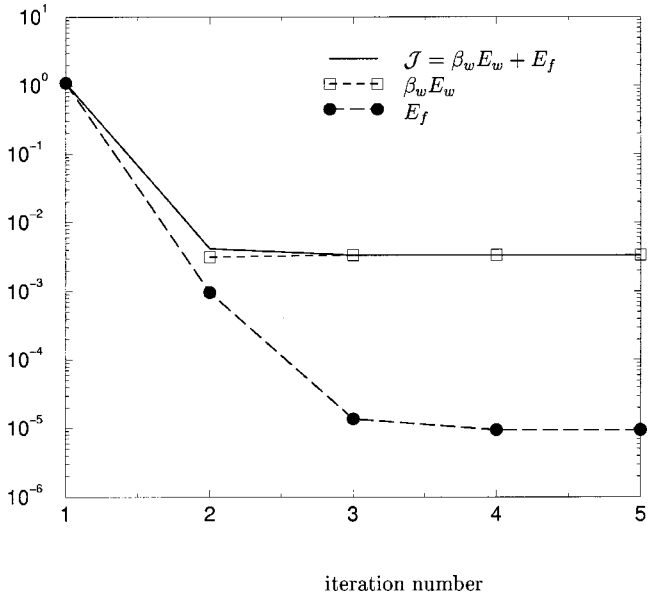

FIG. 3. Behavior of the cost functional and its components during the iterative process; $F=50$, $\beta_w = \beta_w^1$, $\rho = 3\times10^{-3}$.

Note that step 1 is performed for computational convenience only: the approach is in principle, capable of handling the control of arbitrary initial disturbances at the position x_0. In the absence of complete information on the state of the system, i.e., if the initial state is known from noisy flow measurements alone, it is necessary that the control be insensitive to measurement noise and/or state disturbances. Effective control algorithms can then be formulated on the basis of *robust* control theory, a form for which has been recently laid down by Bewley *et al.*[37] There, an iterative scheme not relying on the operator-Riccati setting is proposed that maximizes a cost functional with respect to the noise. Such a formulation could be easily implemented onto our algorithm by inserting an additional step between 5 and 6 to identify saddle point solutions.

B. The numerics

The equations are discretized by finite differences over a uniform x-grid and a stretched y-grid, refined close to the solid boundary; in the streamwise direction a first-order upwind (for the direct problem) or downwind (for the adjoint problem) scheme is employed, whereas the normal-to-the-wall direction is treated by a two-point fourth-order compact scheme. The free-stream boundary is located ten boundary layer thicknesses away from the wall. The closure relations (3) and (14) are enforced at each x station by a Newton–Raphson procedure. The code has been validated against many of the literature cases; for the simulations reported here the grid is typically made up by 125 streamwise and 150 normal points.

TABLE I. Parameters for some of the cases tested.

$F=2\pi f\nu/U_\infty^2\times 10^6$	$R_\delta(x_0)$	$R_\delta(x_f)$	β_w^0	β_w^1
30	350	1750	3.5×10^6	9.34×10^7
50	350	1200	1.4×10^4	4.54×10^4

V. OPTIMAL CONTROL OF THE BLASIUS FLOW

A. Control distributed over the whole streamwise domain

Practical application of the technique is demonstrated here for a flat plate boundary layer forced at a given inflow section x_0 by a two-dimensional TS wave of small amplitude. The disturbance wave is imposed somewhat upstream of the lower branch of the neutral curve (branch I). The second observation point (where one would ideally want to observe a completely damped wave) is close to branch II where, in the absence of control, the amplification of disturbances terminates. In the first set of results reported here, control is applied over the whole domain length.

In Figs. 2 and 3 the evolution of the cost functional within the iterative process is shown, demonstrating the rapid convergence towards the minimum of $\mathcal{J}$ for the two reduced frequencies chosen, $F=30$ and $F=50$ ($F=10^6\,\omega/\mathrm{R}$), and for the values of β_w given in Table I. The disturbance energy at the final station x_f decreases very rapidly from its original (uncontrolled) value E_f^{unc} at iteration 1. The product $\beta_w E_w$ becomes relatively large at convergence, because of the values chosen for the coefficient β_w's; in fact, with a minimal amount of control, and for zero net-mass suction and blowing, the disturbance wave at x_f is reduced by several orders of magnitude. The effect of the relaxation factor is displayed in Fig. 4. The same final values are obtained for the two components of the cost but, as expected, the procedure converges faster towards the global minimum when ρ is larger. The relative reduction at each point in the domain, i.e., the streamwise variation of $E(x)/E^{\mathrm{unc}}(x)$, is reported in Fig. 5 for one of the cases treated. The curve displays a monotonic decrease of the energy with the distance, until a value of the Reynolds number denoted R_I^0 beyond which a plateau is observed, and no further amelioration takes place. Such a value corresponds to an effectively new location of the neutral, branch I, point, as clearly evidenced by Fig. 6 where the energy normalized with respect to its final uncontrolled value is plotted versus the local Reynolds number. The optimal control strategy has, on the one hand, successfully delayed the onset of the instability and, on the other, induced such low perturbation amplitude values as to render them insignificant. The Reynolds number range of amplification in the presence of control is considerably reduced, so that the energy of the disturbance remains tiny even in correspondence of branch II, at the end of the amplification. It is interesting to observe that whereas the branch I neutral point ($\sigma=0$, with σ spatial growth factor based on E) is essentially shifted downstream, the branch II point is unaffected by control for the cases treated (Fig. 7); sufficiently far downstream the

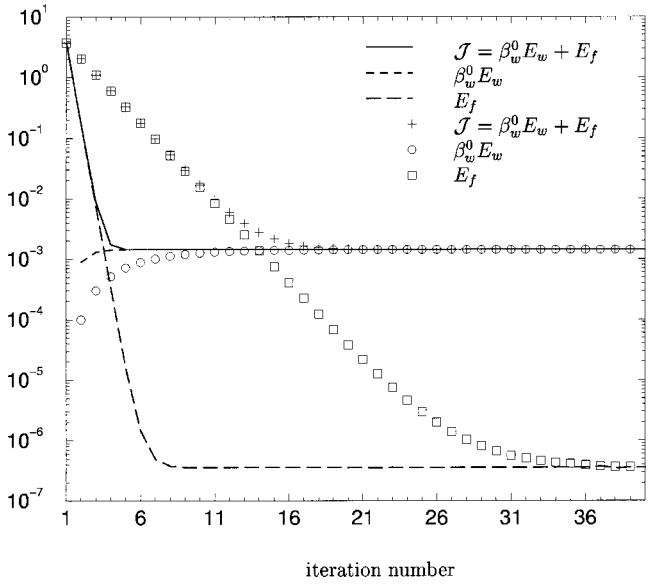

FIG. 4. Influence of the relaxation factor; lines correspond to $\rho=3\times 10^{-4}$ and symbols to $\rho=1\times 10^{-4}$, $F=30$.

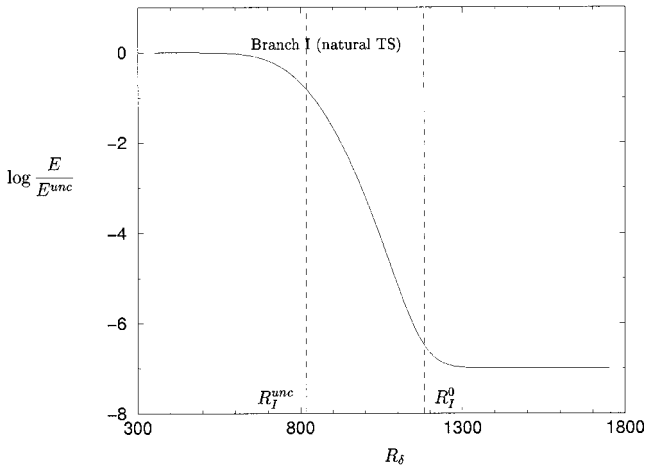

FIG. 5. Relative reduction of E with respect to the uncontrolled case, plotted against the local Reynolds number $\mathrm{R}_\delta=(U_\infty x/\nu)^{1/2}$, for $F=30$ and $\beta_w=\beta_w^0$. $\mathrm{R}_I^{\mathrm{unc}}$ and R_I^0 indicate the location of branch I for the uncontrolled and the controlled cases.

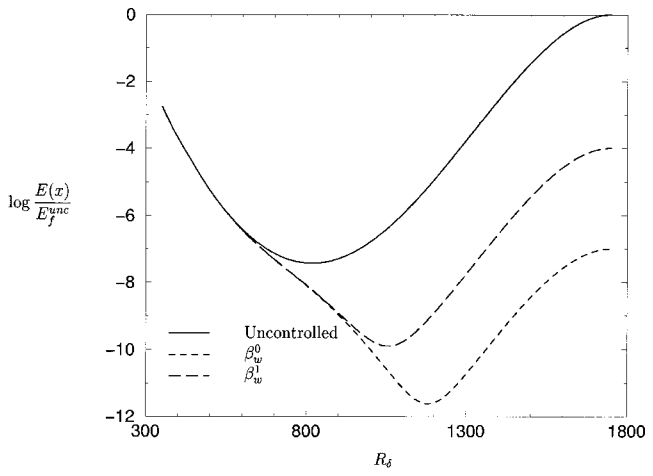

FIG. 6. Energy vs streamwise distance: comparison between uncontrolled and controlled cases, $F=30$.

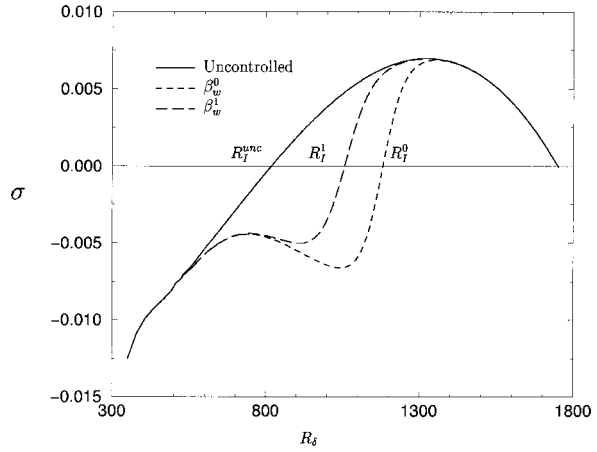

FIG. 7. Growth rate vs streamwise distance; comparison between uncontrolled and controlled cases, $F=30$.

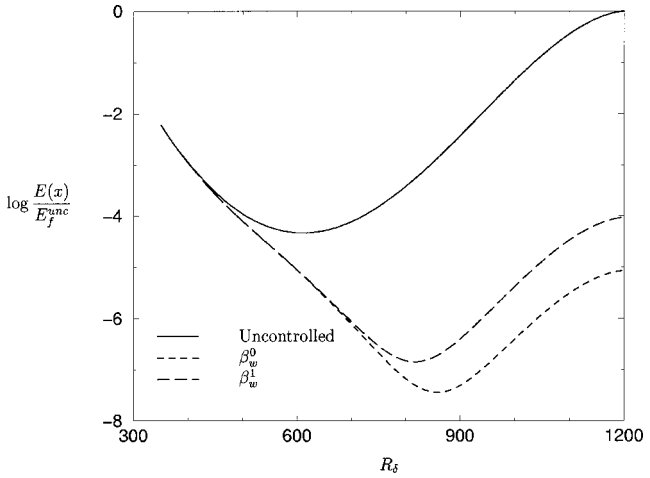

FIG. 9. Energy vs streamwise distance; comparison between uncontrolled and controlled cases, $F=50$.

disturbance wave regains its exponential characteristics (as observed also in previous studies[15]), implying that if the annihilation of the wave is not complete (or nearly complete) interaction phenomena taking place downstream might render the wave superposition approach purposeless.

The advantage of the technique described here is that it does not rely on antiphase wave cancellation but on optimal control theory: thus, although in the present case the end result is identical since a single, infinitesimal wave is being considered and an anti-wave is created by the control, the approach can be extended to nonlinear instabilities where simple wave superposition would fail. We note also that the reduction in disturbance energy by several orders of magnitude achieved here represents a best case, theoretical scenario. Whereas we would not expect such a result in an actual wind tunnel experiment, it is comforting to know that the control found could, in principle, go that far.

The influence of the coefficient β_w weighting the result to the effort expended is shown in Fig. 8; clearly, as β_w decreases less importance is attached to reducing the control energy and, as a consequence, a smaller ratio E_f/E_f^{unc} is attained. For the largest value tested for β_w the disturbance energy reduction is marginal; for smaller β_w than tested one could hope to drive the disturbance amplitude to zero. On practical grounds this is unfeasible since it would require tuning the wall velocity to a required value with infinite precision. As shown in the following, extremely small variations in the control velocity produce order one changes in the final disturbance energy. Figure 9 displays two examples of successful instability delay at $F=50$: in one case a four-order-of-magnitude reduction in final energy is obtained (compared to the uncontrolled case), in the other the reduction is of five orders of magnitude. The modulus of the wall velocity needed in these two cases is shown in Fig. 10: the curves can hardly be discerned from one another, demonstrating the extreme sensitivity of this problem to outer forcing. Not unexpectedly, the optimal control velocity peaks near branch I (of the uncontrolled case), which is the position of maximum receptivity.[28,36] On the other hand, a harmonic forcing near (and upstream of) branch II would be quite ineffective because the wave would have little space (in the streamwise sense) to amplify, before the subsequent quasi-

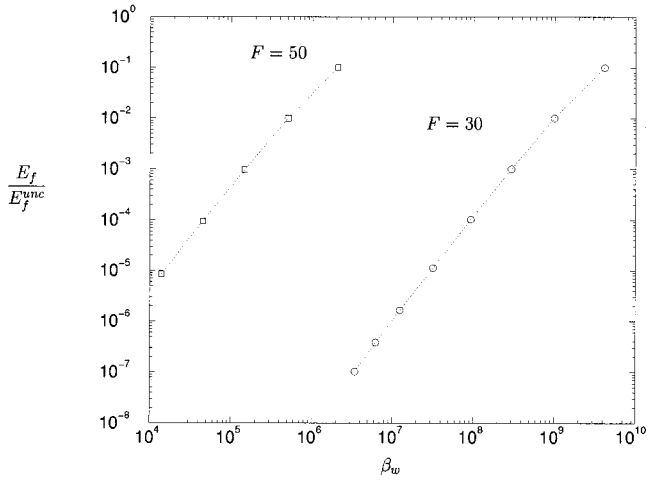

FIG. 8. Link between β_w and E_f/E_f^{unc} for the two frequencies tested.

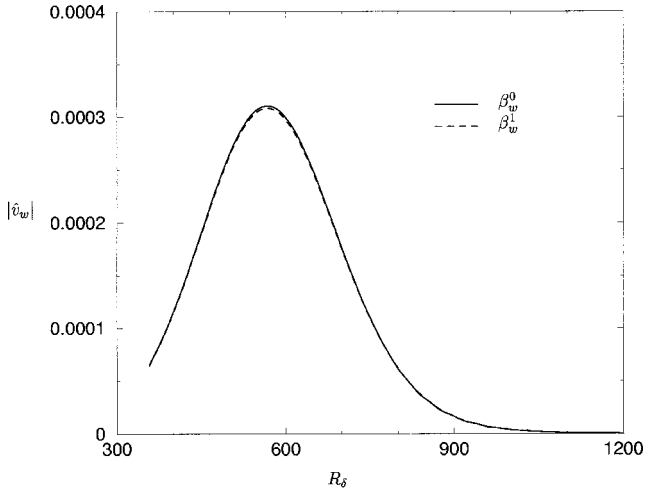

FIG. 10. Modulus of the optimal boundary control for the two cases of Fig. 9.

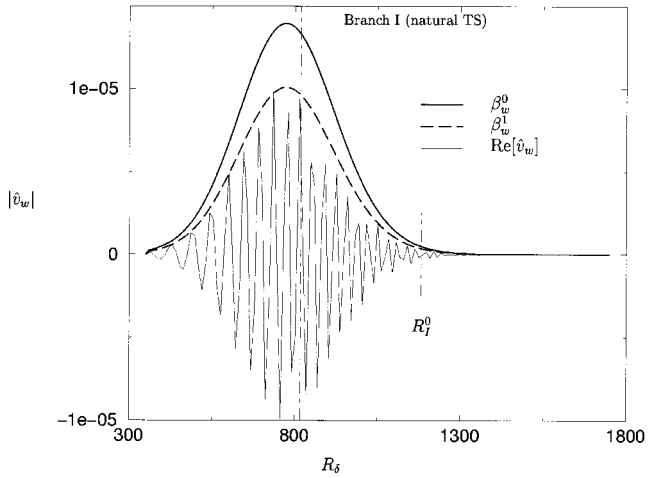

FIG. 11. Optimal control velocity, cases of Fig. 6.

exponential decay. Hence, in this region of very low receptivity the optimal control velocity is of vanishing magnitude.

Figure 11 displays the optimal control for the cases of Fig. 6; the real part of the (complex) wall velocity illustrates the strong streamwise dependence of the control. This result shows why a complete (or nearly complete) cancellation can be achieved in theory, but very hardly in practice. Although this constitutes, today, a technological limit for the kind of active control explored here, current developments in micro- and nano-technologies make it realistic to hope for future actuators to perform with such a degree of precision as to be capable of driving an instability wave to amplitudes two or three orders of magnitude smaller than in the absence of control. In such a case the problem encountered by early experiments and related to nonlinear interactions could be avoided or, at worse, postponed. Hence, the study proposed here constitutes the necessary framework for experiments to be performed once the technology becomes available.

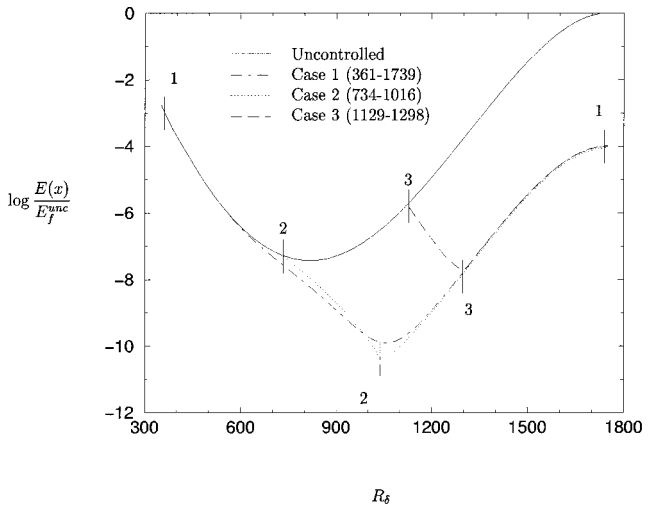

FIG. 12. Streamwise development of the perturbation energy. Comparison between the uncontrolled and some controlled cases; the x-domain over which the control is effected is denoted by the pair of numbers 1, 2, or 3: the corresponding Reynolds number range is indicated in the label to the lines; $F=30$.

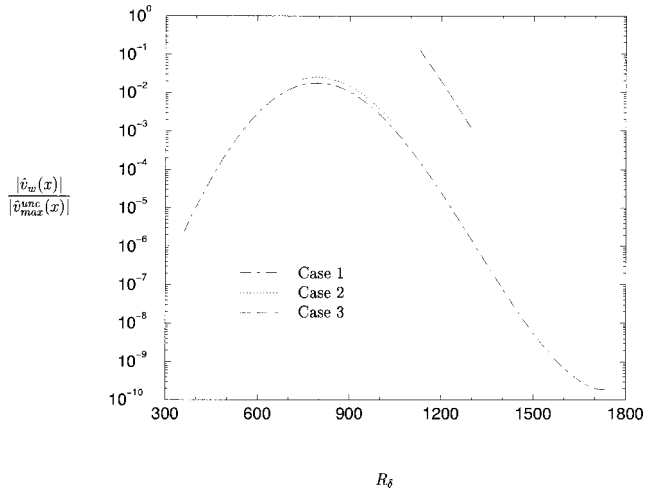

FIG. 13. Optimal control velocity normalized by the largest, local y-velocity disturbance of the uncontrolled case, $F=30$. Control energies are $E_w^1=4.09\times10^{-10}$, $E_w^2=5.64\times10^{-10}$, and $E_w^3=2.74\times10^{-7}$.

B. Control applied at the suction/blowing strip

The spatial extent of the control is one issue of relevance. So far the case has been considered in which the whole streamwise domain is equipped with actuators which blow and suck fluid in and out of the wall. A more realistic scenario, which can be equally well treated by our approach, is that of a spanwise array of actuators of limited streamwise extent: a blowing and suction strip.

A study has been conducted ot the position and length of a suction/blowing strip to ensure efficient operations. Some results are displayed in Fig. 12 for three cases in which the coefficient β_w has been tuned to produce an (almost) identical final disturbance energy. A comparative analysis shows that it is advantageous to place the control strip around the most receptive region, i.e., in the vicinity of branch I. If, for some technological reasons, the control system must be set downstream, the objective may still be reached, but the blowing/suction mass flow (hence the cost of the control) increases, as shown in Fig. 13. In this case, the amplitude of the wall velocity becomes comparable to the maximum, local (in x) value of the vertical disturbance velocity of the uncontrolled case; furthermore, the growth rate of the instability displays rather rapid variations close to the limits of the control domain. These two occurrences might violate one of the underlying assumptions of the PSE, i.e., that of weak nonparallelism. Although here the theory is believed to be still tenable, care must be used in applying the present approach to situations where rapid streamwise variations are induced.

C. The effect of small random errors on the control law

Finally, it is of interest to assess the robustness of our optimal strategy with respect to random noise forcing in the already computed wall velocities, i.e., to determine how efficient the control is when randomly perturbed or inaccurately defined. The case that led to Fig. 2 is used as a reference.

The wall velocity is fixed to $\hat{v}_w^{\mathrm{noisy}}=\hat{v}_w+\epsilon|\hat{v}_w|\mu e^{i\varphi}$

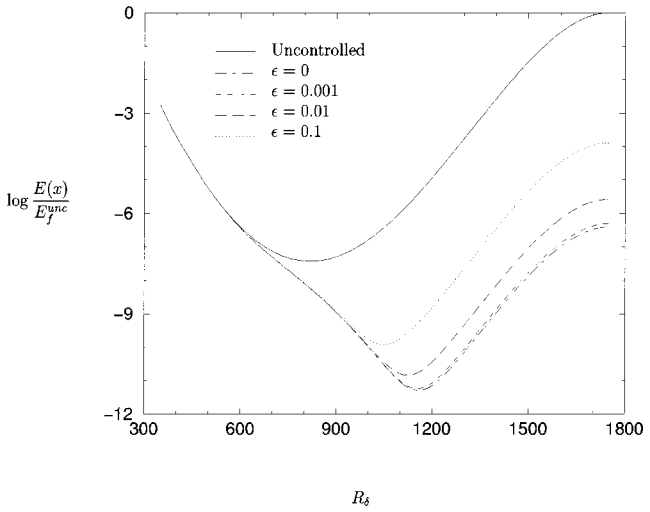

FIG. 14. Disturbance energy for some cases in which the optimal wall velocity is randomly perturbed; $F=30$, $\beta_w=\beta_w^0$.

where $\hat{v}_w$ is the already determined optimal control, μ and φ are random numbers verifying $\mu\in[0,1]$ and $\varphi\in[-\pi,\pi]$, and ϵ is the relative noise level. Figure 14 demonstrates that, as expected, with the increase of ϵ the performances of the controller degrade and the effective branch I position is pushed upstream. A 10% noise level produces a 100-fold increase in energy; on the other hand, the final energy value is still four orders of magnitude smaller than in the case without control. This result is mildly encouraging with respect to accuracy bounds for actuators. The modulus of the relative wall velocity is plotted in Fig. 15 for some significant noise levels. Because of the way they were built, the random disturbances are naturally larger near the peak of $\hat{v}_w$; it is precisely in this region of high receptivity that an operational system must be made to work accurately.

VI. CONCLUDING COMMENTS

A methodology based on optimal control theory has been proposed and validated on some test cases of instability suppression. The methodology is based on the iterative numerical resolution of direct and adjoint systems of nonlocal stability equations, coupled via transfer and optimality conditions.

Optimal (and robust) control theory is reaching such a level of understanding and predictability for flow control situations that its transposition from theory to laboratory experiments is ready. In our work, the control is applied through a zero-net mass flux transpiring wall or strip. The recent introduction of novel concepts for sensors and actuators renders it feasible to conceive the practical realization of the computed control laws in a not-so-distant future in a laboratory environment. Today the limiting point is the extreme sensitivity of the disturbance wave to minute variations in the control, as exemplified in some of the situations studied here. This issue requires a very careful analysis of the interactions outer flow/actuator.

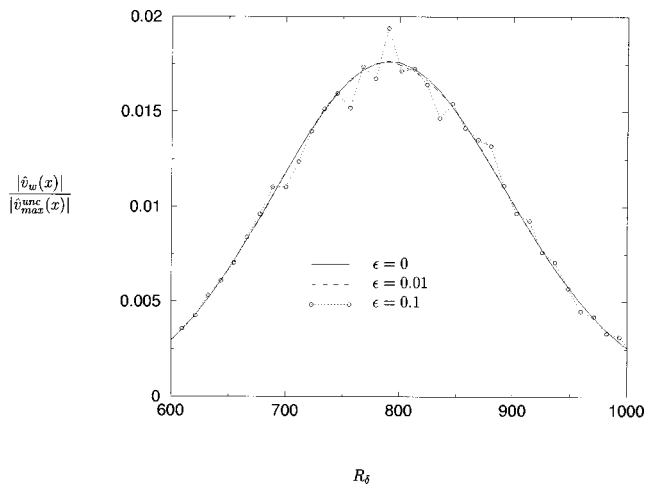

FIG. 15. Close-up of the modulus of the randomly perturbed control velocity; $F=30$, $\beta_w=\beta_w^0$.

APPENDIX: PSE AND APSE MATRICES

The matrices in the two-dimensional operator of Eq. (2) read

$$\mathcal{A}=\begin{bmatrix} V & 0 & 0 \\ 0 & V & 1 \\ 0 & 1 & 0 \end{bmatrix}, \quad \mathcal{B}=\begin{bmatrix} \xi_1 & 0 & 1 \\ 0 & \xi_1 & 0 \\ 1 & 0 & 0 \end{bmatrix}$$

$$\mathcal{C}=\begin{bmatrix} \xi_0+\frac{\partial U}{\partial x} & \frac{\partial U}{\partial y} & i\alpha \\ 0 & \xi_0+\frac{\partial V}{\partial y} & 0 \\ i\alpha & 0 & 0 \end{bmatrix}, \quad \mathcal{D}=\begin{bmatrix} -\frac{1}{R} & 0 & 0 \\ 0 & -\frac{1}{R} & 0 \\ 0 & 0 & 0 \end{bmatrix},$$

where

$$\xi_0=i(\alpha U-\omega)+\frac{\alpha^2}{R}-\frac{i}{R}\frac{d\alpha}{dx} \quad \text{and} \quad \xi_1=U-\frac{2i\alpha}{R}.$$

The adjoint PSE [Eq. (8)] can be written as

$$\mathcal{A}^*\frac{\partial \mathbf{p}}{\partial y}+\mathcal{B}^*\frac{\partial \mathbf{p}}{\partial x}+\mathcal{C}^+\mathbf{p}-\mathcal{D}^*\frac{\partial^2 \mathbf{p}}{\partial y^2}=\left\{\frac{\chi_f}{\overline{\chi_f}}\gamma\frac{\partial u}{\partial x}-\frac{\partial \gamma u}{\partial x}\right\}(1,0,0)^T,$$

$$\mathcal{A}^*=\mathcal{A}; \quad \mathcal{D}^*=\mathcal{D};$$

$$\mathcal{C}^+=\frac{\partial \mathcal{A}^*}{\partial y}+\frac{\partial \mathcal{B}^*}{\partial x}-\mathcal{C}^*=\begin{bmatrix} \xi_2+\frac{\partial V}{\partial y} & 0 & i\overline{\alpha} \\ -\frac{\partial U}{\partial y} & \xi_2-\frac{\partial V}{\partial y} & 0 \\ i\overline{\alpha} & 0 & 0 \end{bmatrix}$$

with

$$\xi_2=i(\overline{\alpha}U-\omega)-\frac{\overline{\alpha}^2}{R}+\frac{i}{R}\frac{d\overline{\alpha}}{dx}$$

and $\mathcal{M}^*=\overline{\mathcal{M}}^T$, $\mathcal{M}$ a generic matrix.

[1]R. Joslin, ''Overview of laminar flow control,'' Technical Report No. NASA/TP-1998-208705, NASA (1998).
[2]R. Joslin, ''Aircraft laminar flow control,'' Annu. Rev. Fluid Mech. **30**, 1 (1998).

[3]M. Gunzburger, ''Adjoint equation-based methods for control problems in incompressible, viscous flows,'' Flow, Turbul. Combust. (in press).
[4]R. W. Milling, ''Tollmien–Schlichting wave cancellation,'' Phys. Fluids **24**, 979 (1981).
[5]G. B. H. W. Liepmann and D. Nosenchuck, ''Control of laminar-instability waves using a new technique,'' J. Fluid Mech. **118**, 187 (1982).
[6]P. J. Strykowski and K. R. Sreenivasan, ''The control of transitional flows,'' AIAA Paper 85-0559 (1985).
[7]L. Maestrello, ''Active transition fixing and control of the boundary layer in air,'' AIAA Paper 85-0564 (1985).
[8]D. M. Ladd and E. W. Hendricks, ''Active control of 2-D instability waves on an axisymmetric body,'' Exp. Fluids **6**, 69 (1988).
[9]A. Thomas, ''The control of boundary-layer transition using a wave superposition principle,'' J. Fluid Mech. **137**, 233 (1983).
[10]V. M. Gilev and V. V. Kozlov, ''Use of small localized wall vibrations for control of transition in the boundary layer,'' Fluid Mech.-Sov. Res. **14**, 50 (1985).
[11]V. M. Gilev and V. V. Kozlov, ''Effect of altering injection and suction on transition in the boundary layer,'' Fluid Mech.-Sov. Res. **16**, 61 (1987).
[12]C. J. Gedney, ''The cancellation of a sound-excited Tollmien–Schlichting wave with plate vibration,'' Phys. Fluids **26**, 1158 (1983).
[13]V. V. Kozlov and V. Y. Levchenko, ''Laminar-turbulent transition control by localized disturbances,'' AIAA Paper 85-0568 (1985).
[14]R. Joslin, R. Nicolaides, F. Erlebacher, M. Hussaini, and M. Gunzburger, ''Active control of instabilities in laminar boundary layer flow. Part II: Use of sensors and spectral controller,'' AIAA J. **33**, 1521 (1995).
[15]R. Joslin, F. Erlebacher, and M. Hussaini, ''Active control of instabilities in laminar boundary layer flow. Overview and concept validation,'' J. Fluids Eng. **118**, 494 (1996).
[16]R. Joslin, M. Gunzburger, R. Nicolaides, F. Erlebacher, and M. Hussaini, ''A methodology for the automated optimal control of flows including transitional flows,'' AIAA J. **35**, 816 (1997).
[17]T. Bewley and S. Liu, ''Optimal and robust control and estimation of linear paths to transition,'' J. Fluid Mech. **365**, 305 (1998).
[18]P. Cathalifaud and P. Luchini, ''Algebraic growth in a boundary layer: optimal control by blowing and suction at the wall,'' Eur. J. Mech. B/Fluids **19**, 469 (2000).
[19]P. Corbett, Ph.D. thesis, Ecole Polytechnique Fédérale de Lausanne, Switzerland, 2000.
[20]F. Bertolotti, T. Herbert, and P. Spalart, ''Linear and nonlinear stability of the Blasius boundary layer,'' J. Fluid Mech. **242**, 441 (1992).
[21]T. Herbert, ''Parabolized stability equations,'' Annu. Rev. Fluid Mech. **29**, 245 (1997).
[22]C. Airiau and G. Casalis, ''Boundary layer linear stability using a system of parabolic equations,'' Rech. Aerosp. **5**, 57 (1993).
[23]C. Airiau and G. Casalis, ''Non linear PSE compared with DNS and experiment,'' in *IUTAM Symposium on Laminar-Turbulent Transition*, Sendai, Japan, edited by R. Kobayashi (Springer, Berlin, 1994), pp. 85–92.
[24]A. Hanifi, ''Local and non-local stability analysis and transition prediction of compressible boundary layer flows,'' Ph.D. thesis and TRITA-MEK Technical Report 1995-12, Royal Institute of Technology, Stockholm, Sweden (1995).
[25]D. Hill, ''Adjoint system and their role in the receptivity problem for boundary layer,'' J. Fluid Mech. **292**, 183 (1995).
[26]A. Tumin, ''Receptivity of pipe Poiseuille flow,'' J. Fluid Mech. **315**, 119 (1996).
[27]P. Luchini and A. Bottaro, ''Görtler vortices: A backward-in-time approach to the receptivity problem,'' J. Fluid Mech. **363**, 1 (1998).
[28]C. Airiau, S. Walther, and A. Bottaro, ''Non-parallel receptivity and the adjoint PSE,'' in *IUTAM Symposium on Laminar-Turbulent Transition*, September 1999, Sedona, AZ, edited by H. Fasel and W. Saric (Springer, Berlin, 2000), pp. 57–62.
[29]S. Collis and A. Dobrinsky, ''Evaluation of adjoint based methods for the prediction of the receptivity,'' in *IUTAM Symposium on Laminar-Turbulent Transition*, September 1999, Sedona, AZ, edited by H. Fasel and W. Saric (Springer, Berlin, 2000), pp. 111–116.
[30]D. Arnal, G. Schrauf, H. Stock, G. Casalis, A. Hanifi, and S. Hein, ''EUROTRANS Final Report,'' Technical Report, European Community (2000).
[31]C. Airiau, Ph.D. thesis, Ecole Nationale Supérieure de l'Aéronautique et de l'Espace, Toulouse, France, 1994.
[32]P. Andersson, D. Henningson, and A. Hanifi, ''On a stabilization procedure for the parabolic stability equations,'' J. Eng. Math. **33**, 311 (1998).
[33]T. Herbert, ''Parabolized stability equations,'' AGARD REPORT (1993).
[34]C. Airiau, ''Non-parallel acoustic receptivity of a Blasius boundary layer using an adjoint approach,'' Flow, Turbul. Combust. (in press).
[35]D. C. Hill, ''Boundary layer receptivity and control,'' Center for Turbulence Research, Annual Research Briefs, Standford University, 1993.
[36]D. Hill, ''Receptivity in non-parallel boundary layers,'' FEDSM97-3108, ASME Fluids Engineering Division Summer Meeting, 1997.
[37]T. Bewley, R. Temam, and M. Ziane, ''A general framework for robust control in fluid mechanics,'' Physica D **138**, 360 (2000).